Counterion Distribution in the Coronal Layer of Polyelectrolyte Diblock Copolymer Micelles

W. Groenewegen,[§] A. Lapp,[†] S. U. Egelhaaf,[‡] and J. R. C. van der Maarel*[,§]

Leiden Institute of Chemistry, Gorlaeus Laboratories, Leiden University, PO Box 9502, 2300 RA Leiden, The Netherlands, Department of Physics and Astronomy, JCMB, University of Edinburgh, Edinburgh EH9 3JZ, United Kingdom, and Laboratoire Léon Brillouin, CE de Saclay, 91191 Gif-sur-Yvette Cedex, France

Received January 20, 2000; Revised Manuscript Received March 29, 2000

ABSTRACT: With a view to describe the structural arrangement of the tetramethylammonium (TMA^+) counterions in simple salt-free aqueous poly(styrene-*block*-acrylic acid) [PS(20)-*b*-PA(85)] solutions, the partial structure factors pertaining to PS−PS, PS−TMA, and TMA−TMA density correlations were obtained with small-angle neutron scattering and isotopic labeling of the counterion. The contributions to the scattering related to the PA-blocks are blanked by contrast matching in water. The copolymers self-assemble with an aggregation number ∼100 into spherical micelles made of a PS-block core, surrounded by a coronal layer formed by the PA-blocks. At the present level of ionization (50%), the PA chains are almost fully stretched in the radial direction away from the core. A comparison of the counterion involved partial structure factors with the previously reported relevant structure factors pertaining to the PA-blocks shows that the counterion distribution along the radius is very close to the one for the segments of the corona-forming blocks. Within a 10% error margin, all counterions are trapped in the coronal layer, and there is no indication for charge annealing effects and/or counterion migration toward the outer corona region.

Introduction

Polyelectrolyte diblock copolymers comprise two linearly attached moieties: a charged amphiphilic and a hydrophobic chain part. Ionic diblocks of poly(styrene-*block*-acrylate) (PS-*b*-PA), with a polyelectrolyte (PA) block length comparable to or larger than the length of the polystyrene (PS) block, associate into spherical micelles made of a hydrophobic PS core, surrounded by a coronal layer formed by the PA-blocks.[1−3] We use the acronym PA to denote the poly(acrylic acid) block, irrespective of the degree of ionization. The critical micelle concentrations of the sodium form of PS-*b*-PA (PS-*b*-NaPA) dispersed in water were reported as a function of block lengths and salt content.[4,5] Hydrodynamic diameters and scaling relations for the core size were derived from dynamic light scattering and transmission electron microscopy (TEM), respectively.[6] These results show that the ionized PA chains in the coronal layer have a highly extended conformation. A near-perfect rodlike stretching (with a scattered intensity $\sim q^{-1}$)[7] of the arms has also been reported for micelles formed by poly(*tert*-butylstyrene-*block*-sodium styrenesulfonate) (PtBS-*b*-NaPSS).[8] This behavior is strikingly different from the situation for uncharged spherical polymer brushes, where the chains take a more compact coiled conformation.[9−13]

In previous work, we have investigated simple salt-free spherical micelles of PS-*b*-PA, in which the corona charge is tuned by titration between almost zero (there is always some residual charge due to the autodissociation) and full charge where every segment carries an ionized group.[14] Detailed structural information about the morphology of the micelles was inferred from small-angle neutron scattering (SANS). The scattering is sensitive to the set of spatial Fourier transforms of the block density correlation functions, i.e., the partial structure factors.[15−17] To describe the structural arrangement of the blocks, the individual partial structure factors pertaining to PS−PS and PA−PA density correlations as well as the composition structure factor were obtained with contrast matching in water. The composition structure factor describes the spatial fluctuation of the *difference* in PS- and PA-block densities and is particularly sensitive to the intramicelle structure.

The PS-blocks were found to form a densely packed spherical core with a radius 4.5 nm and an aggregation number (i.e., the number of self-assembled copolymers per micelle) ∼100; the core structure does not depend on the charge and/or micelle concentration to a significant degree. Because of the high glass temperature (363 K) of the PS-block, the core is in a glassy, metastable state, and once the micelles are formed after cooling below the glass temperature, the structure is fixed. The extension of the PA chains in the coronal layer, and, hence, the micelle radius, was observed to be highly sensitive to the corona charge. At full ionization, the PA chains are almost fully stretched with a density scaling proportional to the inverse second power of the radius away from the core. For lower charge fraction, the results were interpreted in terms of scaling theory for star-branched polyelectrolytes, including the effects of charge annealing (i.e., migration of the charges toward the outer corona region due to the recombination and dissociation balance of the weak polyacid).[18,19]

When the fraction of ionized groups is sufficiently large, the electrostatic screening length is much smaller than the micelle size, and hence, inside the corona there is screening of Coulomb interaction. It is conjectured that the majority of the counterions are confined to the coronal layer, and the concomitant osmotic pressure gives the main contribution to the corona stretching force (osmotic regime).[18−20] Indeed, the derived dimen-

[§] Leiden University.
[†] Laboratoire Léon Brillouin.
[‡] University of Edinburgh.
* Author for correspondence.

10.1021/ma000096h CCC: $19.00
Published on Web 05/03/2000

sion of the micelles was found to be controlled by the balance of the elastic, conformational, stretching forces and the osmotic pressure exerted by the trapped counterions.[14] Furthermore, the scattering data could be consistently analyzed with the assumption that the counterion distribution equals the one for the PA monomers. This assumption was necessary to reduce the number of unknown structure factors. Although there is some indirect evidence, these conjectures regarding the extent to which the counterions are confined to the coronal layer and their distribution along with the radius away from the core need experimental verification.

In the present contribution, we report additional SANS experiments in order to describe the structural arrangement of tetramethylammonium (TMA^+) counterions in the coronal layer of simple salt-free PS-*b*-PA micelles (PS-*b*-TMAPA). The use of TMA^+ counterions rather than Na^+ allows for contrast variation by isotopic labeling of the counterion, while the contributions to the scattering related to the PA-blocks are blanked by contrast matching in water. From the scattering data of samples with different ratios deuterated and hydrogenated TMA, the partial structure factors pertaining to PS−PS (core) and TMA−TMA (counterion) density correlations as well as the composition structure factor are derived. Here, the composition structure factor describes the correlation in the difference of the PS-block and TMA densities and is particularly sensitive to the ordering of the counterions around the core. Half the polyelectrolyte block monomers are ionized (degree of neutralization 0.5), and hence, charge annealing effects and concomitant migration of counterions toward the outer corona region are potentially important. The radial counterion distribution and the extent to which the counterions are trapped in the coronal layer will be gauged from a comparison of the counterion involved partial structure factors with the previously reported relevant factors pertaining to the corona-forming PA-blocks.

Theory

Structure Factors and Contrast Variation. For an A(N_A)-*b*-B(N_B) diblock copolymer, with N_A and N_B the number of monomers of block A and B, respectively, it is convenient to consider the blocks as the elementary scattering units.[21] Every block A is attached to a B-block, and hence, the macroscopic block concentrations exactly match the copolymer concentration $\rho_A = \rho_B = \rho$. The polyelectrolyte B-block is charged to a degree of neutralization DN, and to ensure electroneutrality, the solution contains N_C (=DNN_B) counterions (C) per chain. The coherent part of the solvent corrected SANS intensity reads[7,15]

$$I(q)/\rho = \sum_{i,j} \bar{b}_i \bar{b}_j N_i N_j S_{ij}(q) \qquad (1)$$

where the summation runs over all structure factors $S_{ij}(q)$ pertaining to the density correlations among the solutes ($i = j$ = A, B, and C) and solute pairs ($i \neq j$). In an H_2O/D_2O solvent mixture, the scattering length contrast $\bar{b}_i$ is given by

$$\bar{b}_i = b_i - b_s \bar{\nu}_i/\bar{\nu}_s, \qquad b_s = X(D_2O) b_{D_2O} + (1 - X(D_2O)) b_{H_2O} \qquad (2)$$

with $X(D_2O)$ the D_2O mole fraction. The solute i and solvent s have scattering lengths b_i and b_s and partial molar volumes $\bar{\nu}_i$ and $\bar{\nu}_s$, respectively.

In the present work, the scattering contributions that involve the polyelectrolyte B-block are eliminated by solvent contrast matching of $\bar{b}_B$. This is done by adjusting the solvent scattering length b_s through $X(D_2O)$ in such a way that $\bar{b}_B = 0$. Under this condition, eq 1 is sensitive to the density correlations among the A-block and C-counterions only and takes the form

$$I(q)/\rho = \bar{b}_A^{\,2} N_A^{\,2} S_{AA}(q) + 2\bar{b}_A \bar{b}_C N_A N_C S_{AC}(q) + \bar{b}_C^{\,2} N_C^{\,2} S_{CC}(q) \qquad (3)$$

The structure factors will be unraveled from the intensities by solute contrast variation. For this purpose, a mole fraction $X(^D\text{TMA})$ of the counterions is labeled by deuteration. In a mixture of hydrogenated and deuterated counterions with contrast parameters $\bar{b}_C^H$ and $\bar{b}_C^D$, respectively, the corresponding scattering length contrast takes the average

$$\bar{b}_C = X(^D\text{TMA})\bar{b}_C^D + (1 - X(^D\text{TMA}))\bar{b}_C^H \qquad (4)$$

In the counterion contrast variation according to eq 4, it is assumed that the isotopic labeling has no influence on the structural arrangement of the counterions and/or block segments.

The partial structure factors $S_{ij}(q)$ are the spatial Fourier transforms of the density correlation functions

$$S_{ij}(q) = \frac{1}{\rho}\int_V \mathrm{d}\vec{r}\, \exp(-i\vec{q}\cdot\vec{r})\langle \rho_i(0)\, \rho_j(\vec{r})\rangle \qquad (5)$$

It is of particular interest to construct the composition structure factor

$$S_{AA}(q) - 2S_{AC}(q) + S_{CC}(q) = \frac{1}{\rho}\int_V \mathrm{d}\vec{r}\, \exp(-i\vec{q}\cdot\vec{r})\langle[\rho_A(0) - \rho_C(0)][\rho_A(\vec{r}) - \rho_C(\vec{r})]\rangle \qquad (6)$$

This structure factor displays a maximum at wavelengths of the order of the inverse correlation distance between the A-blocks and the counterions. In the $q \to 0$ limit, the composition structure factor goes to zero because overall electroneutrality prevents macroscopic separation of the counterions and copolymers.

Micelle Model. In a selective solvent, the copolymers form spherical aggregates with a hydrophobic A-block core and a polyelectrolyte B-block corona. As will be shown in the present work, the majority of the counterions are either bound to the polyelectrolyte block or confined to the coronal layer. For an analysis of the scattering data, the micelle is thought to occupy an electroneutral cospherical cell with radius r_{cell}. The cell radius is related to the copolymer concentration and the aggregation number N_{ag} according to $\rho 4\pi\, r_{cell}^3/3 = N_{ag}$. A cloud of counterions surrounds each core, which exactly compensates the corona charge. For a monodisperse system and if the counterion structure is invariant to fluctuations in intermicelle separation, the structure factors eq 5 take the form[15]

$$S_{ij}(q) = \frac{1}{N_{ag}} F_i(q)\, F_j(q)\, S_{cm}(q) \qquad (7)$$

with the form factor amplitude $F_i(q)$ and the micelle center-of-mass structure factor $S_{cm}(q)$. In the absence of interactions between the micelles and/or at sufficiently high values of momentum transfer $S_{cm}(q)$ reduces to unity. Furthermore, $S_{cm}(q)$ is positive definite, since it represents a scattered intensity (i.e., a squared amplitude). The intensities eq 3 can now be expressed in terms of two factors $u_i(q)$ rather than three partial structure factors $S_{ij}(q)$ (i, j = A, C):

$$I(q)/\rho = [\bar{b}_A N_A u_A(q) + \bar{b}_C N_C u_C(q)]^2, \quad u_i(q) = [S_{cm}(q)/N_{ag}]^{1/2} F_i(q) \quad (8)$$

Explicit use of eq 7 in the data analysis according to eq 8 (and, hence, with a concomitant reduction in number of adjustable parameters) results in improved statistical accuracy in the derived structure factors.[14,22] With eq 7, the composition structure factor eq 6 reads

$$S_{AA}(q) - 2S_{AC}(q) + S_{CC}(q) = \frac{1}{N_{ag}}[F_A(q) - F_C(q)]^2 S_{cm}(q) \quad (9)$$

The form factor amplitude $F_i(q)$ can be expressed in terms of the radial core (i = A) or counterion (i = C) density $\rho_i(r)$

$$F_i(q) = \int_{V_{cell}} d\vec{r}\, \exp(-i\vec{q}\cdot\vec{r})\rho_i(\vec{r}) = \int_0^{r_{cell}} dr\, \sin(qr)/(qr) 4\pi r^2 \rho_i(r) \quad (10)$$

The scattering amplitudes are normalized to the aggregation number N_{ag} at $q = 0$.

Scattering Amplitudes. In the case of dense core packing, the radial A-block density is uniform for $0 \le r \le r_c$ and given by $\rho_A(r) 4\pi r_c^3/3 = N_{ag}$ and zero for $r > r_c$, with r_c the core radius. For such uniform profile, the core form factor amplitude takes the form

$$F_A(q) = N_{ag} 3(\sin(qr_c) - qr_c \cos(qr_c))/(qr_c)^3 \quad (11)$$

The segment density in the coronal layer is nonuniform and varies along with the radius away from the core. In previous work, we have adopted an algebraic radial B-block density profile

$$\rho_B(r) = \rho_B(r_c)(r/r_c)^{-\alpha} \qquad r_c \le r \le r_o \quad (12)$$

where $\rho_B(r_c)$ is the density at the core−corona interface and r_o is the outer micelle radius.[14] The value of the density scaling exponent α is determined by the statistics of the polyelectrolyte block. We have shown that for a degree of neutralization exceeding, say, 0.35, the corona is sufficiently charged to induce a linear chain configuration with uniform mass per unit length (i.e., $\alpha = 2$).[14] This can be due to either full stretching of the chains or the formation of radial strings of blobs of uniform size. For the radial counterion distribution $\rho_C(r)$, we will also use algebraic profile eq 12. This implies that we neglect the presumably small fraction of counterions *outside* the coronal layer, and hence, the cell radius is assumed to be equal to the outer micelle radius r_o. The scattering amplitude eq 10 is calculated by numeric integration, despite complex analytical expressions are available.[23]

Table 1. Partial Molar Volumes and Scattering Lengths[a]

solute	$\bar{v}_i$ (cm^3/mol)	b_i (10^{-12} cm)
PAA	48	$1.66 + 1.04X(D_2O)$
PAA$^-$	40	2.03
PS	99	2.33
^{H}TMA	84	−0.89
^{D}TMA	84	11.6
H_2O	18	−0.168
D_2O	18	1.915

[a] $X(D_2O)$ denotes the D_2O mole fraction (effect of exchangeable hydrogen). The polymer data refer to the monomeric unit.

Table 2. Fraction ^{D}TMA [$X(^D$TMA)] and Scattering Length Contrasts in 10^{-12} cm[a]

$X(^D$TMA)	$\bar{b}_{PS}$	$\bar{b}_{PA}$	$\bar{b}_{TMA}$
1	−2.1	0.1	7.8
0.63	−2.1	0.1	3.2
0.45	−2.1	0.1	0.9
0	−2.1	0.1	−4.7

[a] $X(D_2O) = 0.47$.

The algebraic profile eq 12 accounts for the *average* density scaling and neglects *fluctuations*. The effect of fluctuations on the scattering behavior is important when the momentum transfer is of the order of the intermolecular correlation distance within the corona. Furthermore, they contribute to the corona S_{BB} and counterion S_{CC} structure factors only; the cross terms S_{AB} and S_{AC} are unaffected due to the heterodyne interference between the amplitudes scattered by the homogeneous core and the corona or counterions.[24,25]

Experimental Section

Polyelectrolyte Block Copolymer. PS-*b*-NaPA was purchased from Polymer Source Inc., Dorval, Canada. The number-average degrees of polymerization DP of the PS- and PA-blocks are 20 and 85, respectively.[26] PS-*b*-NaPA was brought in the PS-*b*-PAA acid form by dissolving it in 0.1 M HCl and extensive dialysis against water (purified by a Millipore system with conductivity less than 1×10^{-6} Ω^{-1} cm^{-1}). The residual sodium fraction in PS-*b*-PAA was checked by atomic absorption spectroscopy and was less than 0.001. Solutions were prepared by dissolving freeze-dried PS-*b*-PAA in pure water and/or D_2O at 350 K under continuous stirring for 6 h. Furthermore, the solutions were sonicated (Bransonic 5200) for 30 min at room temperature. The sonication power was relatively low (190 W), and hence, there is no risk of damage or decomposition of the block copolymers. Copolymer concentrations were determined by potentiometric titration with NaOH (Titrisol, Merck) and are given in moles of PA-block monomer per dm^3. The polyelectrolyte block was neutralized with tetramethylammonium (^{H}TMA, Merck) and/or deuterated ^{D}TMA-d_{12} (Isotec) hydroxide to a degree of neutralization 0.496. The degree of neutralization is the molar ratio of (added) hydroxide and polyacid monomer.

Scattering. For neutron scattering a set of samples was prepared in solvent mole fraction $X(D_2O) = 0.47$ and polyelectrolyte block monomer concentration 0.092 mol of PA/dm^3. For contrast variation, solutions were made with ^{H}TMA and ^{D}TMA and subsequently mixed by weight to obtain four different ^{H}TMA/^{D}TMA solute compositions. The solvent composition was checked by the values for transmission and with IR spectroscopy. Scattering length contrasts were calculated with eqs 2 and 4 and the parameters in Table 1 and are collected in Table 2. The corona scattering length contrast has been calculated by taking the relevant average of the PAA acid and the dissociated form (PAA$^-$) contrast parameters, $\bar{b}_{PAA}$ and $\bar{b}_{PAA^-}$, respectively. A reference solvent sample with matching H_2O/D_2O composition [$X(D_2O) = 0.47$] was also prepared. Standard quartz sample containers with 0.1 cm (for pure H_2O) or 0.2 cm path length were used.

SANS experiments were done with the PAXY diffractometer, situated on the cold source of the high neutron flux reactor at the Laboratoire Léon Brillouin, CE de Saclay, France. The temperature was kept at 293 K. Samples were measured with two different instrument configurations. A wavelength of 0.8 nm was selected, and the effective distances between the sample and the planar square multidetector (S−D distance) were 1.0 and 5.0 m, respectively. This allows for a momentum transfer range of 0.1−2.6 nm^{-1}. The counting times per sample or solvent were approximately 4 and 7 h for the 1.0 and 5.0 m S−D distance, respectively. Data correction allowed for sample transmission and detector efficiency. The efficiency of the detector was taken into account with the scattering of H_2O. Absolute intensities were obtained by reference to the attenuated direct beam, and the scattering of the pure solvent with the same H_2O/D_2O composition was subtracted. Finally, the data were corrected for a small solute incoherent contribution (∼0.01 cm^{-1}). For very high values of momentum transfer $q >$ 2 nm^{-1}, the intensities become very small, of the order of the statistical error margin 0.005 cm^{-1}.

To facilitate quantitative comparison with earlier data, we have done duplicate measurements of three additional sample sets that were previously investigated with a different instrument (D22, Institute Laue Langevin, Grenoble).[14] These sets contain the same copolymer (i.e., from the same batch) at the same concentration but were in the acid form (DN = 0) or neutralized with alkali to a degree of neutralization DN = 0.1 and 1.0, respectively. Here, the contrast was varied in the solvent in order to obtain the PS core and PA corona structure factors.[14] Apart from a normalization factor, the derived structure factors were in excellent agreement with the previously reported results (not shown). For a perfect absolute match, however, the present data had to be multiplied by a factor of 0.93. This factor was subsequently applied to the scattering data of all samples. Note that an agreement in absolute intensity within 7% is quite gratifying, in view of the notoriously difficult absolute intensity SANS measurements.

Results and Discussion

Data Analysis. For simple salt-free solutions, all ions come from the copolymer, and there are four molecular components: solvent, the PS- and PA-blocks, and tetramethylammonium (TMA^+) counterions. The solvent is treated as a uniform background, and a description of the structure thus requires six partial structure factors. Because of the solvent contrast matching, the PA (=B)-block has approximately zero scattering length contrast and does not contribute to the scattering to any significant degree (Table 2). Accordingly, the intensities of the solvent contrast matched PS-*b*-TMAPA solutions are given by the relevant combination of the three partial structure factors describing the density correlations among the PS (=A)-blocks and TMA^+ (=C) counterions (eq 3).

The PS−PS, PS−TMA, and TMA−TMA partial structure factors are obtained from the scattered intensities of samples with contrast matching in the TMA^+ counterion. Figure 1 displays the intensities of the corresponding 0.1 mol of PA/dm^3 PS-*b*-TMAPA solutions. The samples are neutralized to a degree of neutralization 0.496, and hence, the ratio of the number of PA monomers to the counterions is 2:1. The data collected in the low q region are displayed only, where a strong change in intensity is observed with the variation in the counterion contrast. Note that with ^{D}TMA mole fraction 0.45, the counterion has a relatively small average contrast, and the corresponding intensity is almost proportional to the PS structure factor. The scattering of the sample with the fully deuterated ^{D}TMA is the most intense due to the corresponding large contrast length parameters.

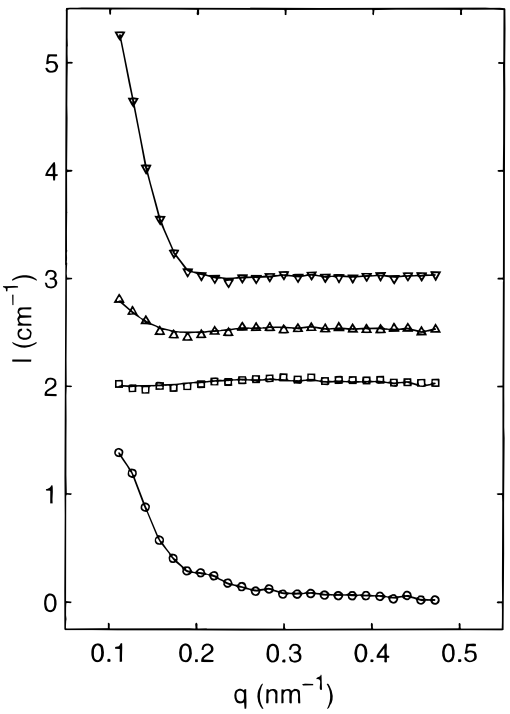

Figure 1. SANS intensity versus momentum transfer from 0.1 mol of PA/dm^3 PS-*b*-TMAPA solutions (DN = 0.5). The ^{D}TMA/^{H}TMA composition is 100, 63, 45, and 0% ^{D}TMA from top to bottom, respectively. The data are shifted along the *y*-axis with 3, 2.5, 2, and 0 cm^{-1}, respectively. The lines represent a two-parameter fit in which the partial structure factors are optimized.

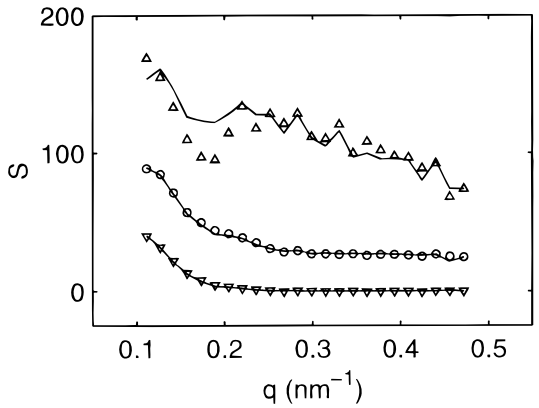

Figure 2. PS−PS (△), PS−TMA (○), and TMA−TMA (▽) partial structure factors in 0.1 mol of PA/dm^3 PS-*b*-TMAPA solutions obtained from a three-parameter fit (DN = 0.5). The solid curves result from a two-parameter fit. The PS−TMA and the TMA−TMA partial structure factors are shifted upward by 25 and 50 units, respectively.

With four experimental intensities and three unknown partial structure factors, the data are overdetermined, and the partial structure factors can be derived by orthogonal factorization in a least-squares sense (i.e., a three-parameter fit to four data points for every q value). The structure factors obtained from the intensities in Figure 1 are shown by the symbols in Figure 2. The statistical accuracy of the PS−PS structure factor is relatively poor, due to the moderate and constant value of the PS scattering length contrast.[27] Note that the decomposition of the experimental intensities into the partial structure factors according to eq 3 is model-free; i.e., no assumptions regarding the

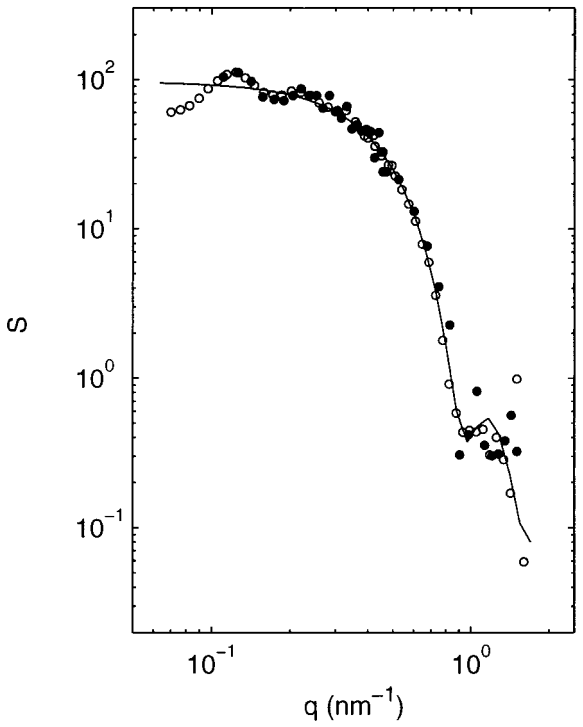

Figure 3. PS−PS core partial structure factor versus momentum transfer: (○) PS-*b*-NaPA, DN = 0.6; (●) PS-*b*-TMAPA, DN = 0.5. The polyelectrolyte block concentrations are 0.1 mol of PA/dm^3. The curve represents a fit with the form factor of a uniform sphere.

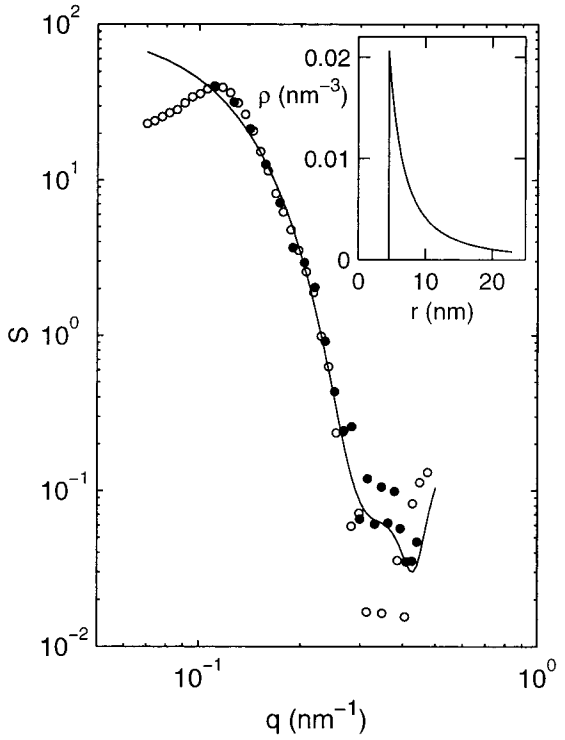

Figure 4. Comparison of the PA−PA corona and the TMA−TMA counterion partial structure factors: (○) PA−PA partial structure factor in PS-*b*-NaPA solutions (DN = 0.6); (●) TMA−TMA partial structure factor in PS-*b*-TMAPA solutions (DN = 0.5). The polyelectrolyte block concentrations are 0.1 mol of PA/dm^3. The solid curve represents the intramicelle form factor with density scaling exponent α = 2. The inset displays the radial density.

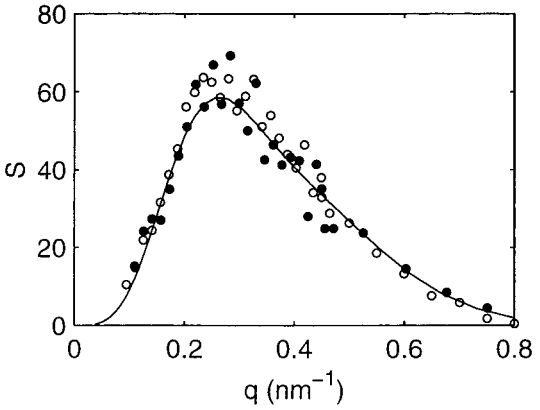

Figure 5. As in Figure 4, but for the composition structure factors: (○) PS−PS − 2PS−PA + PA−PA composition structure factor in PS-*b*-NaPA solutions (DN = 0.6); (●) PS−PS − 2PS−TMA + TMA−TMA composition structure factor in PS-*b*-TMAPA solutions (DN = 0.5).

morphology of the association structures have been made. In previous transmission electron microscopy and SANS work, it was shown that the micelles are spherical and rather monodisperse in size.[14] The statistical accuracy of the derived partial structure factors can be improved if the spherical shape of the micelles is recognized.

For monodisperse spherical micelles, the partial structure factors can be expressed as a product of terms involving the radial core and/or counterion profiles and a term describing the micelle center-of-mass structure factor (eq 7). As shown by eq 8, the intensities can now be expressed in terms of two unknown factors $u_i(q)$ rather than three partial structure factors $S_{ij}(q)$ (i, j = PS, TMA). With a nonlinear least-squares procedure, the two factors $u_i(q)$ were fitted to the data, and the partial structure factors were reconstructed according to $S_{ij}(q) = u_i(q)u_j(q)$. The fitted intensities and the derived partial structure factors are given by the solid curves in Figures 1 and 2, respectively. The statistical accuracy in the structure factors has now improved, while the general behavior agrees with the results obtained from the model-free three-parameter fit. This agreement strongly supports our hypothesis that correlations between intermicelle separation and counterion structure can be neglected and is particularly gratifying in the case of the TMA−TMA and the PS−TMA terms. The latter two structure factors describe the TMA density correlations and, hence, are sensitive to the counterion distribution in the coronal layer.

The data were analyzed with the two-parameter procedure, and the PS−PS (core) and TMA−TMA (counterion) partial structure factors are shown in Figures 3 and 4, respectively. Both structure factors should extrapolate to the micelle aggregation number in the $q \rightarrow 0$ limit and the absence of intermicelle interference. The PS−TMA cross partial structure factor is not displayed. Instead, the composition structure factor eq 6 is more informative and is displayed in Figure 5. We have also included in Figures 3−5 the relevant structure factors pertaining to the density correlations among the PS-block and the (corona) PA-block. The latter results were obtained in previous work with PS- and PA-block contrast variation in the water.[14] Furthermore, they refer to the same copolymer at the same micelle concentration, but the polyelectrolyte block was neutralized with alkali to a degree 0.6. Unfortunately, the degrees of neutralization in the PS-*b*-NaPA and PS-*b*-TMAPA solutions are a little different (0.6 vs

0.5, respectively). However, this difference in DN results in a minor change in the outer micelle radius of the order of 3%, which is less than the estimated error margin 5%.[14]

Core Structure. It is clear from Figure 3 that the structure factor pertaining to the core-forming PS-blocks in the PS-*b*-TMAPA solutions matches the previously obtained one for PS-*b*-NaPA. Despite that these results were obtained with different instruments and with a different experimental methodology (solute vs solvent contrast matching, respectively), the agreement is gratifying and confirms the quantitative agreement in data normalization. The PS−PS partial structure factors are compared to the resolution broadened form factor of a uniformly dense sphere [i.e., according to eq 7 with the square of the relevant scattering amplitude eq 11 and $S_{cm}(q)$ set to unity].[14] In the low q range, the data deviate from the form factor. A correlation peak at $q_{max} = 0.12$ nm^{-1} and oscillatory behavior at higher q values are observed, because of interference between cores pertaining to different micelles. Beyond the correlation peak, the latter interference effects become progressively less important, and the structure factor reflects the internal structure of the core. In the comparison of the sphere form factor with the PS−PS data, the aggregation number N_{ag} and the core radius r_c were optimized and take the values 97 and 4.5 nm, respectively.[14]

As shown in ref 14, the core radius and the aggregation number comply with a densely packed and solvent excluded core formed by the PS-blocks. The present results show that the use of TMA^+ (which is necessary for the determination of the counterion structure) rather than Na^+ counterions has no effect on the core structure. This is perhaps not a surprising result, because the counterion exchange and the measurements were done at room temperature, which is well below the glass temperature of PS (363 K). Accordingly, the core is in a glassy, metastable state, and once the micelles are formed, the core structure is invariant to the corona charge regulation, micelle concentration and/or counterion exchange. We will further focus on the counterion distribution, which is reflected by the TMA−TMA (counterion) and the composition structure factors.

Counterion Structure. The TMA−TMA partial structure factor is displayed and compared with the PA−PA (corona) partial structure factor in Figure 4. In previous work it was shown that the little difference in the degrees of neutralization (0.6 vs 0.5 for PS-*b*-NaPA and PS-*b*-TMAPA, respectively) has no effect on the corona structure factor beyond experimental accuracy.[14] The TMA−TMA and PA−PA structure factors show an almost perfect match in both the scaling with momentum transfer and absolute normalization.[28] This observation immediately confirms that the distribution of the counterions along the radius is very close to the one for the monomers of the corona-forming blocks. The ratio of the counterion and corona structure factors is, hence, q-independent with an average value 0.99 ± 0.10. Accordingly, the quantitative agreement in absolute normalization shows that, within a 10% error margin, *all* counterions are confined to the coronal region. This supports our conjecture that, to a good approximation, the cell radius r_{cell} equals the outer micelle radius r_o and that the micelle is almost electroneutral.

The counterion and corona structure factors display a correlation peak at finite wavelengths, which is due to the ordering of the micelles. For higher values of momentum transfer, the interference between different micelles becomes progressively less important (i.e., $S_{cm}(q) \approx 1$), and the structure factors $S_{ii}(q)$ may be compared with the single-micelle form factor $F_i(q)^2/N_{ag}$ (i = PA, TMA). Because of the steep decrease of the structure factors with increasing q, a possible intracorona (fluctuation) peak is beyond detection.[14,29] We now compare the data with the form factor, which was calculated with eq 7 (with $S_{cm}(q)$ set to unity) and the scattering amplitude eq 10 with numeric integration of the algebraic density profile eq 12. The result with density scaling exponent $\alpha = 2$ and outer micelle radius $r_o = 23$ nm is also displayed in Figure 4 (the density profile is displayed in the inset). The micelle radius was optimized in the fit of the form factor to the PA−PA data (DN = 0.6).[14] A density scaling exponent $\alpha = 2$ is relevant in the case of either full stretching of the chains or the formation of radial strings of blobs of uniform size. Note that the value of the radius for the fully stretched PA amounts to 25.5 nm, as estimated from the sum of the core radius and the contour length of the PA-block. Accordingly, the PA chains in the coronal layer take an almost fully stretched configuration. It is clear from Figure 4 that the counterion structure factor can be described by the same radial density profile as for the segments of the corona-forming blocks. Further evidence for the similarity of the counterion and the corona profiles will be presented in the following, where the composition structure factor is discussed.

The composition structure factor eq 6 describes the spatial fluctuation of the difference in PS-block and TMA densities and is particularly sensitive to the ordering of the counterions around the core. The result is displayed in Figure 5, together with the previously obtained composition structure factor pertaining to the ordering of corona-forming blocks. The theoretical composition form factor expression eq 9 with $S_{cm}(q)$ set to unity is also displayed in Figure 5. In the calculation of the composition form factor, the core and cell (or outer micelle) radii, as well as the aggregation number, were fixed at their values obtained from the PS−PS (core) and PA−PA (corona) data (DN = 0.6). With a density scaling exponent $\alpha = 2$, the theoretical form factor expression predicts the ordering satisfactorily. In particular, deviations from the single-micelle calculation are less prominent in comparison with the situation for the TMA−TMA or PA−PA structure factors. This is because the composition structure factor takes its maximum value beyond the intermicelle correlation peak. In the region of the correlation peak (at $q \approx 0.12$ nm^{-1}) the composition factor already approaches zero.

The composition structure factors display a maximum at wavelengths of the order of the inverse correlation distance of the counterions or PA monomers from the core. Furthermore, they should go to zero for $q \to 0$, because of overall electroneutrality and/or the chemical attachment of the PA- and PS-blocks. (The Coulomb interaction prevents macroscopic separation of the counterions from the micelle.) Both composition structure factors, pertaining to the core−counterion and core−corona correlations, respectively, agree in qualitative and quantitative behavior. The equivalence in the position of the maximum and long wavelength ($q \to 0$) behavior shows that the correlation distance of the counterions from the core is very close to the one for the PA monomers. Accordingly, to a good approximation,

the corona charge is compensated by the counterions within the coronal layer, and there is no indication for counterion ordering over larger distances or preferential migration of the counterions toward the outer corona region.

Conclusions

For a description of the structural arrangement of the counterions, we have obtained the PS−PS, TMA−TMA, and the composition structure factors for a sample with half the PA-block monomers ionized. The structure factors were obtained with isotopic labeling of the counterion, and the contributions to the scattering related to the PA-blocks were blanked by contrast matching in the solvent. All new results are compared to the relevant structure factors pertaining to the density correlations among the PS- and PA-blocks. The latter data were obtained in previous work (with solvent contrast matching), and they refer to the same copolymer, but neutralized with alkali.[14] All data were interpreted with a heterogeneous micelle model, i.e., a self-assembled spherical morphology consisting of a PS-block core, surrounded by a coronal layer formed by the PA-blocks. The correlations among the micelles are beyond the scope of the present work and have not been discussed.

From the PS−PS structure factor, it was observed that, below the PS glass temperature, the TMA^+/Na^+ counterion exchange procedure has no effect on the structure of the core. Furthermore, the quantitative agreement with the previous results confirmed that the data are correctly normalized. (The normalization was facilitated by duplicate measurements.) From a comparison with the theoretical form factor, it follows that the core has a spherical shape with a radius 4.5 nm and an aggregation number ∼100.

The quantitative and qualitative agreement of the counterion involved structure factors with the relevant structure factors pertaining to the corona-forming PA-blocks shows that the distribution of the counterions along the radius is very close to the one for the PA monomers. Furthermore, this agreement implies that within a 10% error margin all counterions are confined to the coronal layer or bound to the polyelectrolyte block. This conclusion is also supported by the X-ray reflectivity from a poly(ethylethylene-*block*-styrenesulfonate) monolayer at the air/water interface, where the majority of the counterions was observed to be associated with the polyelectrolyte block.[30] Accordingly, the micelles are almost electroneutral, but one should realize that due to the large aggregation number a relatively small fraction of free counterions is already sufficient to introduce a significant net charge. The concomitant osmotic pressure exerted by the trapped counterions gives, hence, the main contribution to the corona stretching force, and the micelles are in the osmotic regime.[18,19] Indeed, the micelle radius as a function of the corona charge was found to comply with the corresponding scaling result for polyelectrolyte stars.[14] The PA chains are almost fully stretched with a density scaling proportional to the inverse second power of the radius away from the core. The counterions follow this density scaling, and there are no indications for counterion ordering over larger distances or migration of counterions toward the outer corona region. This is also in accordance with our previous results, where charge annealing effects were found to be significant at very low corona charge fraction only (DN $\lesssim$ 0.1).[14]

Acknowledgment. We acknowledge the Laboratoire Léon Brillouin in providing the neutron research facilities. The scattering experiment was financially supported by the European Commission through the TMR-LSF (Training and Mobility of Researchers−Access to Large Scale Facilities Program, Contract ERB CHGE CT 95 0043).

References and Notes

(1) Zhang, L.; Eisenberg, A. *Science* **1995**, *268*, 1728.
(2) Moffitt, M.; Khougaz, K.; Eisenberg, A. *Acc. Chem. Res.* **1996**, *29*, 95.
(3) Cameron, N. S.; Corbierre, M. K.; Eisenberg, A. *Can. J. Chem.* **1999**, *77*, 1311.
(4) Astafieva, I.; Zhong, X. F.; Eisenberg, A. *Macromolecules* **1993**, *26*, 7339.
(5) Astafieva, I.; Khougaz, K.; Eisenberg, A. *Macromolecules* **1995**, *28*, 7127.
(6) Zhang, L.; Barlow, R. J.; Eisenberg, A. *Macromolecules* **1995**, *28*, 6055.
(7) Here, q denotes the momentum transfer and is defined by the wavelength λ of the radiation and the angle θ between the incident and scattered beam according to $q = 4\pi/\lambda \sin(\theta/2)$.
(8) Guenoun, P.; Muller, F.; Delsanti, M.; Auvray, L.; Chen, Y. J.; Mays, J. W.; Tirrell, M. *Phys. Rev. Lett.* **1998**, *81*, 3872.
(9) Daoud, M.; Cotton, J.-P. *J. Phys.* (*Paris*) **1982**, *43*, 531.
(10) Dozier, W. D.; Huang, J. S.; Fetters, L. J. *Macromolecules* **1991**, *24*, 2810.
(11) Cogan, K. A.; Gast, A. P.; Capel, M. *Macromolecules* **1991**, *24*, 6512.
(12) Förster, S.; Wenz, E.; Lindner, P. *Phys. Rev. Lett.* **1996**, *77*, 95.
(13) Marques, C. M.; Izzo, D.; Charitat, T.; Mendes, E. *Eur. Phys. J. B* **1998**, *3*, 353.
(14) Groenewegen, W.; Egelhaaf, S. U.; Lapp, A.; van der Maarel, J. R. C. *Macromolecules* **2000**, *33*, 3283.
(15) Lovesey, S. W. *Theory of Neutron Scattering from Condensed Matter*; Oxford University Press: Oxford, 1984; Vol. 1.
(16) Higgins, J. S.; Benoit, H. C. *Polymers and Neutron Scattering*; Oxford University Press: Oxford, 1994.
(17) Rawiso, M. *J. Phys. IV* **1999**, *9*, Pr1−147.
(18) Borisov, O. V. *J. Phys. II* **1996**, *6*, 1.
(19) Borisov, O. V.; Zhulina, E. B. *Eur. Phys. J. B* **1998**, *4*, 205.
(20) Misra, S.; Mattice, W. L.; Napper, D. H. *Macromolecules* **1994**, *27*, 7090.
(21) Please note that this definition differs from the situation for homopolymers, where the monomer is usually considered to be the elementary scattering unit.
(22) Zakharova, S. S.; Egelhaaf, S. U.; Bhuiyan, L. B.; Outhwaite, C. W.; Bratko, D.; van der Maarel, J. R. C. *J. Chem. Phys.* **1999**, *111*, 10706.
(23) Förster, S.; Burger, C. *Macromolecules* **1998**, *31*, 879.
(24) Auvray, L. *C. R. Acad. Sci. Paris* **1986**, *302*, 859.
(25) Auvray, L.; de Gennes, P. G. *Europhys. Lett.* **1986**, *2*, 647.
(26) The degree of polymerization of the PS-block was determined by the manufacturer with size exclusion chromatography. For the PA-block, use of the quoted degree of polymerization (N_{PA} = 120, determined from the ratio of the aromatic to the aliphatic protons in the NMR spectrum of the poly(styrene-*b-tert*-butyl acrylate) precursor) gives incorrect normalization of the PA−PA structure factor and incorrect limiting low q behavior of the composition structure factor. In ref 14, N_{PA} was optimized by satisfying the normalization constraints and takes the value 85 monomers per copolymer chain.
(27) The PA scattering length contrast is small and also constant for all samples (0.1×10^{-12} cm, see Table 2). The counterion structure factor is unaffected by a small, residual scattering from the PA-block density correlations, since the former is obtained from the modulation of the intensities with contrast variation in TMA. However, the PA contributes to the PS involved structure factors to an insignificant degree.
(28) Note that the structure factors are normalized, and factors related to the counterion and polyelectrolyte block concentrations have been accounted for.
(29) Heinrich, M.; Rawiso, M.; Zilliox, J. G.; Lesieur, P.; Simon, J. P. *Eur. Phys. J. E*, in press.
(30) Ahrens, H.; Förster, S.; Helm, C. A. *Phys. Rev. Lett.* **1998**, *81*, 4172.

MA000096H